

MAL-PDT inhibits oral precancerous cells and lesions via autophagic cell death

Yen-Yun Wang¹ | Yuk-Kwan Chen^{1,2,3} | Chu-Sung Hu^{4,5} | Ling-Yi Xiao⁶ |
Wan-Ling Huang⁶ | Tsung-Chen Chi⁶ | Kuang-Hung Cheng^{7,8} | Yun-Ming Wang^{9,10} |
Shyng-Shiou F. Yuan^{6,11,12,13} 

¹School of Dentistry, College of Dental Medicine, Kaohsiung Medical University, Kaohsiung, Taiwan

²Division of Oral Pathology & Maxillofacial Radiology, Kaohsiung Medical University Hospital, Kaohsiung, Taiwan

³Oral & Maxillofacial Imaging Center, College of Dental Medicine, Kaohsiung Medical University, Kaohsiung, Taiwan

⁴Department of Dermatology, College of Medicine, Kaohsiung Medical University, Kaohsiung, Taiwan

⁵Department of Dermatology, Kaohsiung Medical University Hospital, Kaohsiung Medical University, Kaohsiung, Taiwan

⁶Department of Medical Research, Kaohsiung Medical University Hospital, Kaohsiung Medical University, Kaohsiung, Taiwan

⁷Institute of Biomedical Sciences, National Sun Yat-Sen University, Kaohsiung, Taiwan

⁸Department of Medical Laboratory Science and Biotechnology, Kaohsiung Medical University, Kaohsiung, Taiwan

⁹Department of Biological Science and Technology, Institute of Molecular Medicine and Bioengineering, National Chiao Tung University, Hsinchu, Taiwan

¹⁰Department of Biomedical Science and Environmental Biology, Kaohsiung Medical University, Kaohsiung, Taiwan

¹¹Translational Research Center, Kaohsiung Medical University Hospital, Kaohsiung Medical University, Kaohsiung, Taiwan

¹²Department of Obstetrics and Gynecology, Kaohsiung Medical University Hospital, Kaohsiung Medical University, Kaohsiung, Taiwan

¹³School of Medicine, College of Medicine, Kaohsiung Medical University, Kaohsiung, Taiwan

Correspondence

Shyng-Shiou F. Yuan, Translational Research Center, Kaohsiung Medical University Hospital, Kaohsiung Medical University, Kaohsiung, Taiwan.

Email: yuanssf@kmu.edu.tw and

Yun-Ming Wang, Department of Biological Science and Technology, Institute of Molecular Medicine and Bioengineering, National Chiao Tung University, Hsinchu, Taiwan.

Email: ymwang@mail.nctu.edu.tw

Funding information

Kaohsiung Medical University (KMU-Q107010), NSYSU-KMU JOINT RESEARCH, (#NSYSUKMU 107-P019); Ministry of Education for Center For Intelligent Drug Systems and Smart Bio-devices (IDS2B) from The Featured Areas Research Center Program within the framework of the Higher Education Sprout Project; the Ministry of Health and Welfare (MOHW107-TDU-B-212-114016, Health and welfare surcharge of tobacco products) of Taiwan, Grant/Award Number: MOHW107-TDU-B-212-114016

Abstract

Background: Oral cancer is a common cancer with a high mortality rate. While surgery is the most effective treatment for oral cancer, it frequently causes deformity and dysfunction in the orofacial region. In this study, methyl aminolevulinate photodynamic therapy (MAL-PDT) as a prevention tool against progression of precancerous lesion to oral cancer was explored.

Methods: For in vitro studies, we evaluated the effects of MAL-PDT on viability of DOK oral precancerous cells by XTT, cell morphology by TEM, and intracellular signaling pathways by flow cytometry, Western blotting, and immunofluorescence. For in vivo study, DMBA was used to induce oral precancerous lesions in hamsters followed by MAL-PDT treatment. We measured tumor size and body weight weekly. After sacrifice, buccal pouch lesions were processed for H&E stain and immunohistochemistry analysis.

Results: MAL-PDT induced autophagic cell death in DOK oral precancerous cells. The autophagy-related markers LC3II and p62/SQSTM1 and autophagosome formation in DOK cells were increased after MAL-PDT treatment. In vivo, Metvix[®]-PDT treatment decreased tumor growth and enhanced LC3II expression in hamster buccal pouch tumors induced by DMBA.



Conclusions: Our in vitro and in vivo results suggest that MAL-PDT may provide an effective therapy for oral precancerous lesions through induction of autophagic cell death.

KEY WORDS

autophagy, methyl aminolevulinate, oral cancer, oral precancerous lesion, photodynamic therapy

1 | INTRODUCTION

Oral cancer is a common cancer worldwide, with a higher incidence in men (Gupta et al., 2016). It is commonly diagnosed at advanced stages with lymph node metastasis and deep invasion into local structures and is associated with high mortality rate (Godeny, 2014; Guneri & Epstein, 2014). Oral precancerous lesions may progress into oral cancer if not detected and treated at the precancerous stage. Therefore, early diagnosis and early treatment are essential for improving the survival rate and life quality of oral cancer patients.

Photodynamic therapy (PDT) is a minimally invasive and clinically approved treatment for various cancers including oral cancer (van Straten, Mashayekhi, Bruijn, Oliveira, & Robinson, 2017). Compared with surgery, the benefits of topical PDT include lack of long-term side effects, less invasiveness, quick and convenient treatment time, and little or no scar formation (Tierney, Eide, Jacobsen, & Ozog, 2008; Wang et al., 2001). PDT uses a light-sensitive compound, which adheres to precancerous and cancer areas (Rigual et al., 2013; Yamamoto et al., 2013). A photochemical reaction occurs between a light excitable molecule (photosensitizer) and molecular oxygen (Bicalho et al., 2013; Hsu, Yang, Chiang, Lee, & Tseng, 2012; van Straten et al., 2017). PDT may induce tumor cell death directly by stimulating reactive oxygen species (ROS) production, or indirectly by damage to tumor vasculature and activation of immune responses against tumor cells (Agostinis et al., 2011).

The most commonly used topical PDT drugs in clinical practice are 5-aminolevulinic acid (ALA) and methyl aminolevulinate (MAL) (Kim, Jung, & Park, 2015). Although ALA is effective in many cancer types, its hydrophilic characteristic is a barrier for fusion with the cell membrane. MAL, a methyl ester of ALA, is a lipophilic compound which results in greater permeability into tissues and cells. Hence, MAL may enhance the intracellular accumulation of protoporphyrin IX (PpIX) in tumor cells (Cohen & Lee, 2016; Gaullier et al., 1997). However, MAL-PDT was originally used in the treatment of skin cancer (Fargnoli & Peris, 2015; Wen, Li, & Hamblin, 2017) and its efficacy in oral precancerous lesions is unclear. Therefore, in this study, we explored the therapeutic efficacy of MAL-PDT in oral precancerous lesions and investigated the underlying mechanisms.

2 | MATERIALS AND METHODS

2.1 | Cell lines

DOK oral precancerous cells were cultured in DMEM supplemented with 10% fetal bovine serum, 100 U/ml penicillin, 100 µg/ml streptomycin, 2 mM glutamine, and 5 µg/ml hydrocortisone. Oral cancer

cells (Ca9-22) were grown in Eagle's minimal essential medium with 2 mM glutamine and 10% fetal bovine serum. Both cell lines were incubated at 37°C with 5% CO₂.

2.2 | Animal model

The animal studies were approved by the Institutional Animal Care and Use Committee (IACUC no. 104010) of Kaohsiung Medical University, Taiwan. Animal experiments were approved by the Laboratory Animal Ethics Committee of Kaohsiung Medical University and were conducted in accordance with the Animal Research: Reporting In Vivo Experiments (ARRIVE) guidelines. Twenty-three outbred male Syrian golden hamsters (*Mesocricetus auratus*), weighing 80–100 g each at the start of the experiment, were randomly assigned into one of the following four groups to test the efficacy of topical Metvix[®] followed by PDT. Hamsters were injected with Lysol before being sacrificed by CO₂ asphyxiation. Tumor size was measured once a week, and tumor volume was calculated according to a standard formula: (width² × length)/2.

2.3 | Photosensitizer and PDT

In this study, methyl aminolevulinate (MAL, Sigma-Aldrich, USA) was used for in vitro studies and 16% MAL topical cream (Metvix[®], Galderma, Paris, France) was used in vivo. The protocol for red light stimulation of PDT was 6 J/cm² for 90 s. The total time period of Metvix[®]-PDT was 860 s. Red light stimulation of Metvix[®]-PDT was performed at 200 mW/cm² (lighting for 120 s and then stop for 120 s for three cycles, followed by lighting for 140 s). For the experimental group (Group D), DMBA-treated hamsters were treated with Metvix[®]-PDT once a week for 2 weeks. The photosensitizer was manufactured by Photocure, The Bladder Cancer Company (Aktilite[®], Galderma Benelux, Rotterdam, the Netherlands).

2.4 | XTT cell viability assay

DOK and Ca9-22 cells were seeded at a density of 4.5 × 10³ cells/well onto 96-well plates and allowed to attach overnight. For MAL-PDT studies, the cells were incubated with MAL for 16 hr, treated with/without rapamycin or 3-methyladenine (3-MA), and then exposed to red light at 6 J/cm² for 90 s. Cell viability was evaluated by the XTT colorimetric assay. Following treatment, 2,3-Bis(2-methoxy-4-nitro-5-sulfophenyl)-2H-tetrazolium-5-carboxanilide (Sigma-Aldrich, USA) and PMS (*N*-methyl dibenzopyrazine methyl sulfate, Sigma-Aldrich, USA) were added into each well. Absorbance was

determined by a spectrophotometer at 475 nm with a reference wavelength at 660 nm. The relative numbers of viable cells as compared to the numbers of cells in the untreated group were presented as percentage of viable cells using the following formula: cell viability (%) = A_{475} of treated cells/ A_{475} of untreated cells.

2.5 | Transmission electron microscopy (TEM)

DOK cells were treated with MAL-PDT for 48 hr and fixed with 2.5% glutaraldehyde and 2.5% formaldehyde for 2 hr. Then, the cells were reacted with 1% OSO_4 for 1 hr, washed with 5% sucrose, and incubated with 2% uranyl acetate for 1 hr. Subsequently, cells were dehydrated by adding gradually increased concentrations of ethanol (50% to 100%), incubated with acetone/Spurr's resin (1:1) for 30 min, incubated with 100% Spurr's resin for 30 min, and then embedded at 60°C for 24 hr. Ultra-thin sections were prepared and visualized by electron microscopy (JEM-1200EX, JEOL, Tokyo, Japan).

2.6 | Immunoblotting analysis

After treatment with MAL-PDT for 48 hr, DOK and Ca9-22 cells were harvested and lysed. Equal amounts of proteins were subjected to SDS-PAGE and transferred onto polyvinylidene difluoride (PVDF) membranes. The PVDF membranes were blocked with 5% skim milk at room temperature for 1 hr, incubated with primary antibodies, washed with 1X TBST (Tris-buffered saline with Tween-20), and then incubated with horseradish peroxidase-conjugated secondary antibodies (1:5,000 dilution, Thermo Scientific) at room temperature for 1 hr. Immunoreactive proteins were detected by Enhanced chemiluminescence (SuperSignal™ West Femto Maximum Sensitivity Substrate, Thermo Scientific). Finally, the immunoblots were imaged by ChemiDoc XRS+ System (Bio-Rad, USA) and quantified by Image Lab™ software (Bio-Rad, USA). The primary antibodies used for immunoblotting analysis included caspase-3 (Novus Biologicals, Littleton, CO, USA), caspase-7, caspase-9, cleaved-PARP, LC3B (Cell Signaling Tech., Danvers, MA, USA), γ H2AX, p62/SQSTM1, and β -actin (Genetex, Irvine, CA).

2.7 | Immunofluorescent staining

Cells were seeded at 8,000 cells/well in eight-well chamber slides (Millicell EZ Slide) and incubated for 24 hr before treatment. After incubation with MAL for 16 hr followed by red light at $6 J/cm^2$ for 90 s, cells were fixed immediately in 4% paraformaldehyde at room temperature for 15 min, permeabilized at $-20^\circ C$ for 10 min, and blocked with 5% bovine serum albumin for 1 hr at room temperature. Cells were incubated with LC3B antibody (Cell Signaling Tech., Danvers, MA, USA) for 2 hr at room temperature, reacted with Alexa Fluor 488-conjugated secondary antibody (Life Technologies, Grand Island, NY, USA) for 1 hr, and then counterstained with DAPI for 1 min at room temperature. Images were captured with a Laser confocal microscope (FV1000, Olympus, Japan) with excitation at 330–385 nm and emission at 470–495 nm.

2.8 | Acridine orange staining

Formation of acidic vesicular organelles (AVOs), a morphological characteristic of autophagy, was determined by acridine orange staining (Thome et al., 2016). Cells were stained with 1 $\mu g/ml$ acridine orange (AO) for 15 min and counterstained with DAPI for 1 min at room temperature. AO labels the acidic compartments with red fluorescence, and the intensity of red fluorescence is directly proportional to the acidification of the cellular compartments. Images were captured with a Nikon Eclipse Ti-S-inverted microscope with excitation at 330–385 nm and emission at 530–550 nm. For flow cytometry analysis, cells were treated with MAL-PDT for 48 hr, incubated with 0.5 mg/ml AO for 15 min, and then analyzed by flow cytometry.

2.9 | Autophagosome detection

The formation of autophagosomes and autolysosomes in DOK cells was determined with the Promo™ Autophagy Tandem Sensor RFP-GFP-LC3B Kit (Invitrogen, Carlsbad, CA, USA) according to the manufacturer's protocols. The RFP-GFP-LC3B sensor allows the visualization of LC3B-positive, neutral pH autophagosomes with green fluorescence (GFP), and LC3B-positive, acidic pH autolysosomes with red fluorescence (RFP). Cells were cultured on coverslips and incubated with 6 μl of BacMam Reagent containing the RFP-GFP-LC3B sensor overnight. The cells were then treated with MAL-PDT for 48 hr. After rinsing with 1 \times PBS and nuclear staining with DAPI, the coverslips were mounted with VECTASHIELD (Vector Laboratories, Burlingame, CA) and imaged by a Laser confocal microscope (FV1000, Olympus, Japan) with excitation at 330–385 nm, 470–495 nm, and 530–550 emission filter.

2.10 | Immunohistochemistry and hematoxylin & eosin staining

Oral mucosa tissues from the buccal pouches of hamsters were excised and fixed in 10% neutral-buffered formalin solution for 24 hr, followed by histological processing and paraffin embedding. Tissue sections (4 μm thick) were obtained and mounted on glass slides for further experiments. Immunohistochemical staining for autophagic markers LC3B-GFP and p62/SQSTM1 was performed using the fully automated Bond-Max system in accordance with the manufacturer's instructions (Leica Microsystems, Wetzlar, Germany). For quantification of p62/SQSTM1 staining, the percentage of positively stained tumor cells was graded semiquantitatively according to the following categories: 0 (0%–4%), 1 (5%–24%), 2 (25%–49%), 3 (50%–74%), or 4 (75%–100%). In addition, the global staining intensity was scored as 0 (negative), 1 (weak), 2 (moderate), or 3 (strong). The total immunostaining score was calculated as the percentage of positively stained cells multiplied by the global staining intensity. In addition, hamster oral tissues were stained with hematoxylin and eosin.

2.11 | Annexin V/PI staining

Ca9-22 cells were treated with MAL-PDT and stained with Annexin V-FITC and PI from BD Biosciences (Franklin Lakes, NJ) for 15 min. Apoptosis was analyzed by flow cytometry (FC 500 MCL, Beckman Coulter, USA).

2.12 | Colony formation

Twenty-four hours after MAL-PDT treatment, Ca9-22 cells were trypsinized and seeded at a density of 500 cells/well in 96-well plates. Ten days later, the cells were stained with 0.5% crystal violet (Merck Millipore, USA).

2.13 | Terminal deoxynucleotidyl transferase (TdT)-mediated dUTP nick-end labeling (TUNEL)

TUNEL assay was performed using an Apoptosis Detection Kit (Invitrogen, Carlsbad, CA, USA) according to the manufacturer's instructions. Cell apoptosis was determined by flow cytometry and light microscopy. TUNEL-positive nuclei (with intense brown staining) were counted in three randomly selected microscopic fields (200 \times) and were expressed as a percentage of the total number of nuclei counted.

2.14 | ROS detection

Cells were treated with MAL-PDT and then stained in the dark with 10 μ M dihydroethidium (DHE) or DCF-DA for 20 min at 37°C. The level of intracellular ROS was determined by flow cytometry. Mean fluorescence intensity was determined using FlowJo software.

2.15 | Statistical analysis

All statistical analyses were done using the JMP 9.0 statistical package. Quantitative data were presented as mean \pm SD from three independent experiments. Differences between experimental groups were determined by one-way analysis of variance (ANOVA) with post hoc Tukey's test for multiple comparisons. *p* Value less than 0.05 was regarded to be statistically significant.

3 | RESULTS

3.1 | MAL-PDT-induced autophagic cell death of DOK cells in vitro

The cytotoxic activity of MAL-PDT on oral precancerous cells and the underlying mechanisms were first addressed in vitro using DOK oral precancerous cells. MAL-PDT, but not MAL or PDT alone, induced a significant decrease in the viability of DOK cells, as determined by the XTT cell viability assay (Figure 1a). However, the expression levels of superoxide indicator dihydroethidium (DHE) (Supporting Information Figure S1A), pro-apoptotic markers (Supporting

Information Figure S1B), and Annexin V-positivity (Supporting Information Figure S1C) in DOK cells were all unchanged after MAL-PDT treatment, suggesting that apoptosis was not involved in MAL-PDT-induced DOK cell death. Under light microscopy, accumulation of cytoplasmic vacuoles in DOK cells was observed after MAL-PDT treatment, an observation which raises the possibility of autophagic cell death (Figure 1b). Indeed, double-layered autophagosomes were observed in DOK cells following MAL-PDT treatment under transmission electron microscopy (TEM) (Figure 1c).

LC3 is a well-documented marker for autophagosomes (Tanida I, 2011; Schaaf, Keulers, Vooijs, & Rouschop, 2016). After the GFP-LC3 expression vector was transfected into DOK cells, LC3 puncta were counted under fluorescence microscopy. As shown in Figure 2a, MAL-PDT treatment stimulated the formation of LC3II puncta. Furthermore, the protein expression levels of p62/SQSTM1 and LC3II (both are markers for autophagosomes) in DOK cells were increased upon MAL-PDT treatment (Figure 2b). Acridine orange (AO) staining was used to identify autophagic cell death under fluorescence microscopy (Thome et al., 2016), and we observed significantly increased AVO formation after MAL-PDT treatment (Figure 2c,d). We also used Premo™ Autophagy Tandem Sensor RFP-GFP-LC3B (Invitrogen, Carlsbad, CA, USA), which allows for enhanced analysis of the maturation of autophagosomes to autolysosomes. By combining an acid-sensitive GFP with an acid-insensitive RFP, the change from autophagosomes (neutral pH) to autolysosomes (with an acidic pH) can be visualized by detecting the specific loss of green fluorescence, leaving only red fluorescence. Indeed, we observed an increase in yellowish LC3II puncta in the cytosol of DOK cells after treatment with MAL-PDT (Figure 2e,f).

To further confirm the involvement of autophagy in MAL-PDT-induced cell death, DOK cells were co-treated with 3-MA (an autophagy inhibitor) and MAL-PDT, and cell viability was analyzed. An increase in DOK cell viability was observed after co-treatment of cells with 3-MA and MAL-PDT, indicating that autophagy was indeed involved in MAL-PDT-induced cell death in DOK cells (Figure 2g). In agreement with this result, the expression level of LC3II was also decreased after 3-MA co-treatment (Supporting Information Figure S2A). Conversely, co-treatment of cells with rapamycin (an autophagy activator) and MAL-PDT led to enhanced cell death in DOK cells (Figure 2h). Of note, the LC3II level remained high, though no longer upregulated, after rapamycin and MAL-PDT co-treatment (Supporting Information Figure S2B).

3.2 | MAL-PDT-induced apoptotic cell death of Ca9-22 in vitro and in vivo

The autophagic cell death in MAL-PDT-treated DOK oral precancerous cells was further tested in oral cancer cells, Ca9-22. Under light microscopy, we did not observe cytosolic vacuoles in Ca9-22 cells upon MAL-PDT treatment (Figure 3a). However, MAL-PDT still led to decreased cell viability and colony formation in Ca9-22 cells (Figure 3b,c). Further analysis showed that the fluorescence intensity

of DHE (Figure 3d), the percentage of apoptotic cells (Figure 3e), the expression of pro-apoptotic proteins (Figure 3f), and the percentage of TUNEL⁺ cells (Figure 3g,h) were all increased in Ca9-22 cells upon MAL-PDT treatment. In addition, increased TUNEL⁺ cells were observed in hamster oral cancer tissues after Metvix[®]-PDT treatment (Figure 3i).

3.3 | METVIX[®]-PDT significantly suppressed tumor growth and induced autophagic cell death in DMBA-induced oral precancerous lesions

In this study, 7,12-dimethylbenz[a]anthracene (DMBA) was applied on the buccal pouch of hamsters to induce oral precancerous

lesions (Chen & Lin, 2010; Shklar, Eisenberg, & Flynn, 1979), followed by Metvix[®]-PDT treatment with the time scheme illustrated in Figure 4a. The control group (Group A, *n* = 2) consisted of hamsters without any treatment, neither DMBA nor Metvix[®]-PDT. For the experimental groups (Groups B–D), the left buccal pouch was painted 10 times with 0.5% DMBA (in mineral oil) three times per week for 8 weeks using the no. 4 sable-hair brush. Hamsters in Group B (*n* = 5) were treated with DMBA but not Metvix[®]-PDT and were sacrificed at the 13th week. Hamsters in Group C were treated with DMBA but not Metvix[®]-PDT and were sacrificed at the 11th week. Hamsters in Group D (*n* = 11) were treated with DMBA followed by Metvix[®]-PDT treatment. Both the control group (Group A) and experimental groups (Groups B and D) were

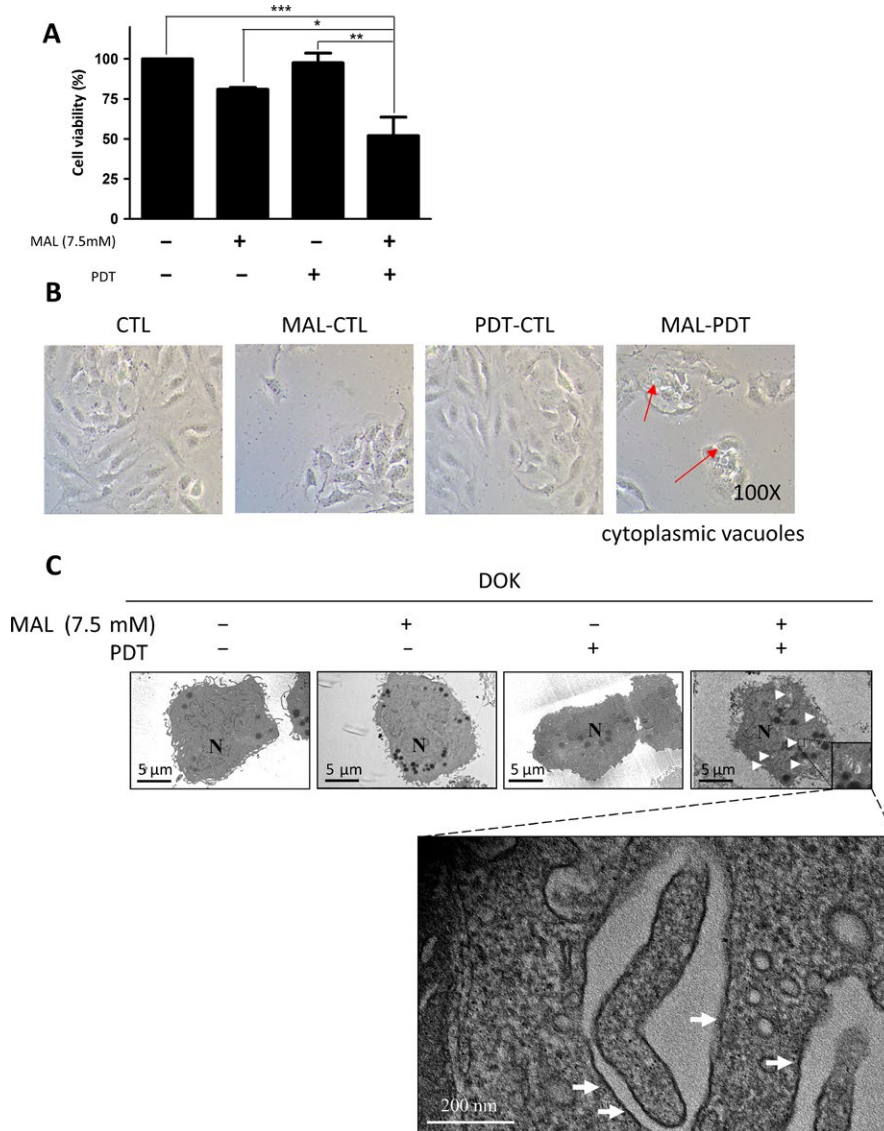


FIGURE 1 Cytotoxic effect of MAL-PDT on DOK oral precancerous cells. (a) Effect of MAL-PDT on DOK cell viability. Cell viability was assessed at 48 hr after PDT by the XTT colorimetric assay. (b) Microscopic findings in DOK cells after MAL-PDT treatment (magnification $\times 100$). DOK cells were divided into 4 groups including cells without any treatment (CTL), cells treated with MAL only (MAL-CTL), cells treated with PDT only (PDT-CTL), and cells treated with MAL-PDT (MAL-PDT). (c) Autophagosome formation in DOK cells as visualized by TEM. Autophagosomes are characterized by double-layered structures containing engulfed mitochondria and cytoplasmic material (arrows) (magnification $\times 15,000$). * $p < 0.05$, ** $p < 0.01$, *** $p < 0.001$, compared with the indicated group by one-way ANOVA [Colour figure can be viewed at wileyonlinelibrary.com]

euthanized at the 13th week. For verification of precancerous lesions, five DMBA-treated hamsters (Group C) were euthanized at the 11th week. The representative photographs for the DMBA-untreated group (Group A), DMBA control group (Group B), DMBA-treated hamsters before Metvix[®]-PDT treatment (Group C), and DMBA-treated hamsters after Metvix[®]-PDT treatment (Group D) are shown in Figure 4b. H&E stains for oral mucosa tissues from each group are shown in Figure 4c. Compared with

Group B, the average tumor volume for Group D was significantly smaller at 1 and 2 weeks after Metvix[®]-PDT treatment (Figure 4d and Supporting Information Table S1). Of note, no difference in body weight was observed in DMBA-treated hamsters with or without Metvix[®]-PDT treatment (Supporting Information Figure S3A). Moreover, PDT alone or Metvix[®] alone did not cause any histological changes in normal oral epithelium or precancerous lesions (Supporting Information Figure S3B,C).

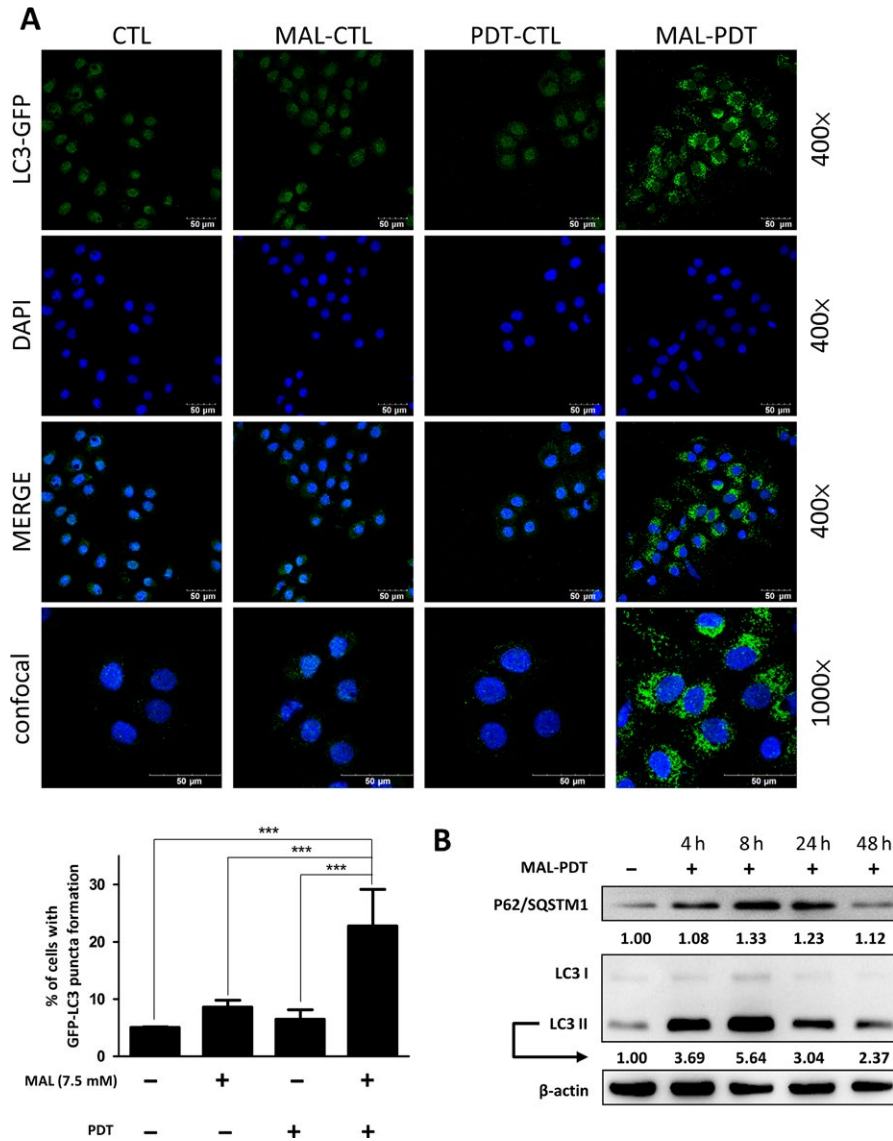


FIGURE 2 Effects of MAL-PDT on autophagy in DOK oral precancerous cells. (a) MAL-PDT-induced autophagy in DOK cells, as analyzed by cytosolic GFP-LC3 puncta. The autophagosomes were labeled with GFP-LC3 puncta (green), and the nuclei were labeled with DAPI (blue). (b) The expression levels of autophagy proteins, p62/SQSTM1 and LC3II, in oral precancerous cells, as determined by immunoblotting. The expression of β -actin was used as the internal control. The results are representative of three separate experiments. (c) DOK cells were treated with MAL-PDT followed by acridine orange (AO) staining at 48 hr after PDT to identify autophagic cells under fluorescence microscopy (magnification $\times 100$). (d) The effect of MAL-PDT on the accumulation of acidic vesicular organelles (AVOs) in DOK cells was determined at 48 hr after PDT by flow cytometry. (e) The effect of MAL-PDT on the formation of autophagosomes and autolysosomes in DOK cells was determined by RFP-GFP-LC3B protein localization with fluorescence microscopy and confocal microscopy (magnification $\times 1,000$). (f) Autophagosomes in MAL-PDT-treated DOK cells were detected by the autophagy detection kit. (g) DOK cell viability after co-treatment with MAL-PDT and 20 μ M 3-MA for 48 hr, as measured by the XTT assay. (h) DOK cell viability after co-treatment with MAL-PDT and 0.5 nM rapamycin for 48 hr, as measured by the XTT assay. *** $p < 0.001$, compared with the indicated group by one-way ANOVA [Colour figure can be viewed at wileyonlinelibrary.com]

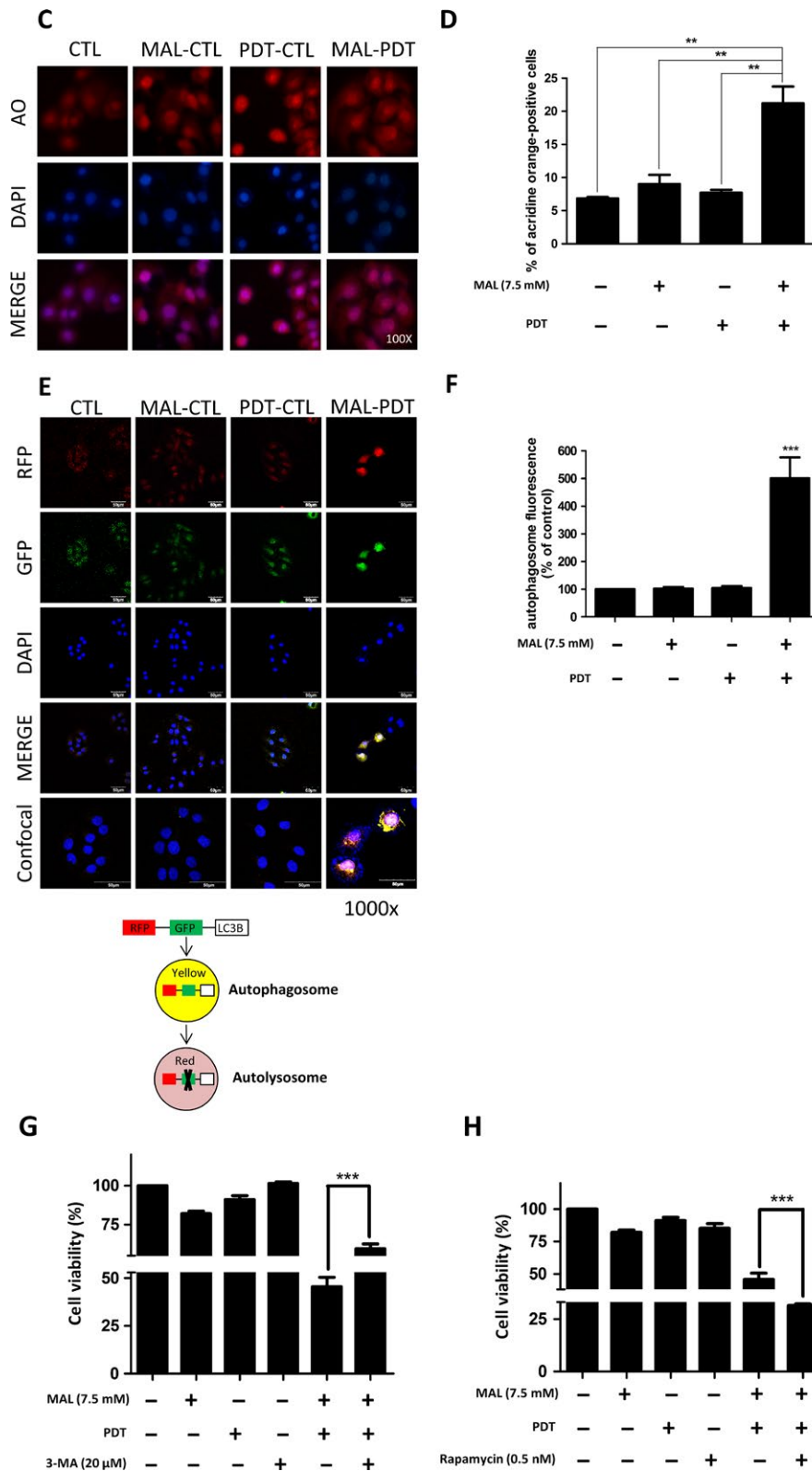


FIGURE 2 Continued

To address the involvement of autophagy in the suppression of precancerous tumor growth following MAL-PDT treatment *in vivo*, H&E and immunofluorescent staining for GFP-LC3 puncta formation were performed. Decreased tumor mass (Figure 5a) and increased

LC3 puncta formation (Figure 5b,c) were observed after Metvix[®]-PDT treatment. Furthermore, the accumulation of p62/SQSTM1 in the tumor lesions was decreased, while TUNEL staining was not evident after Metvix[®]-PDT treatment (Figure 5d,e).

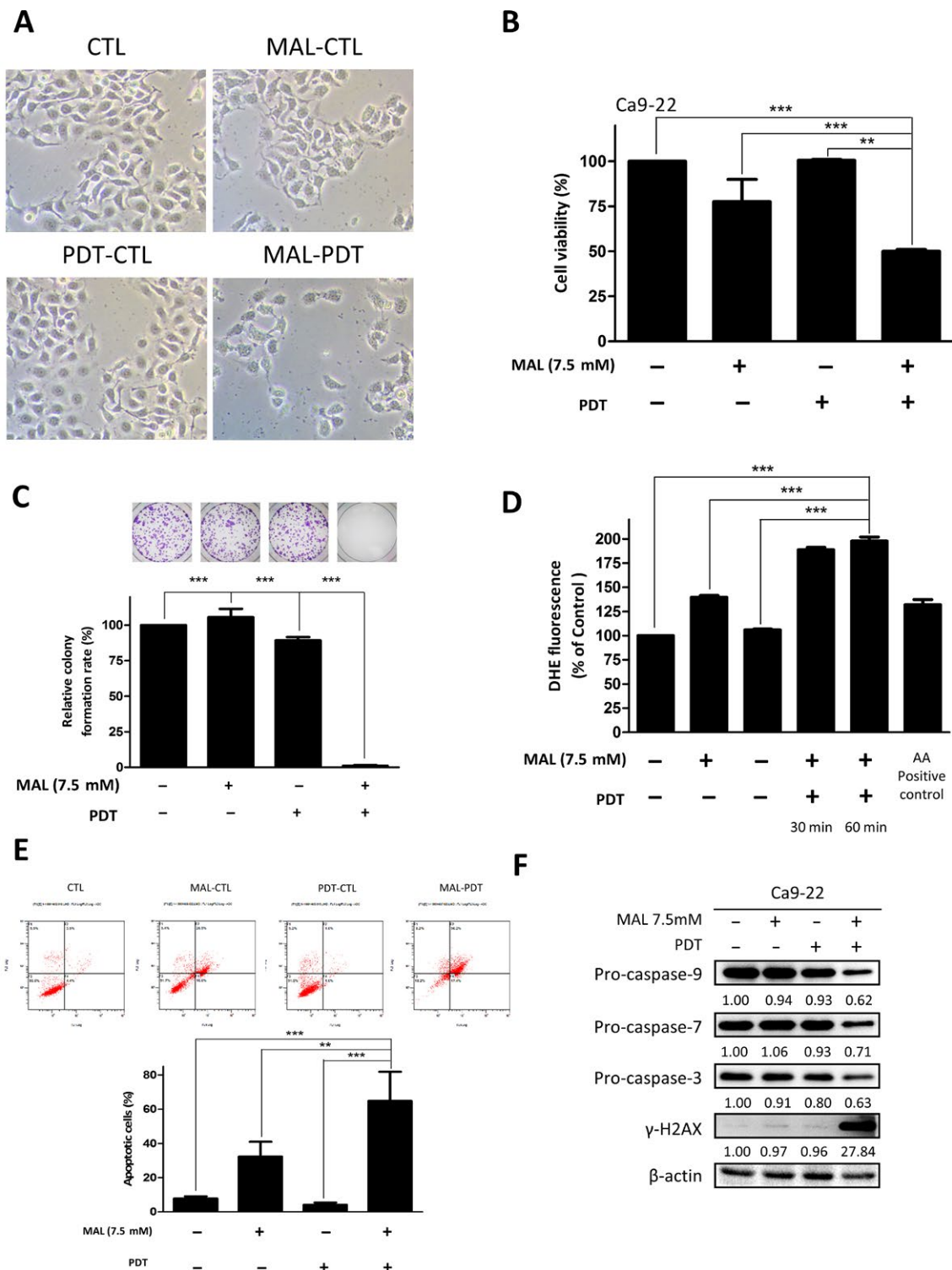
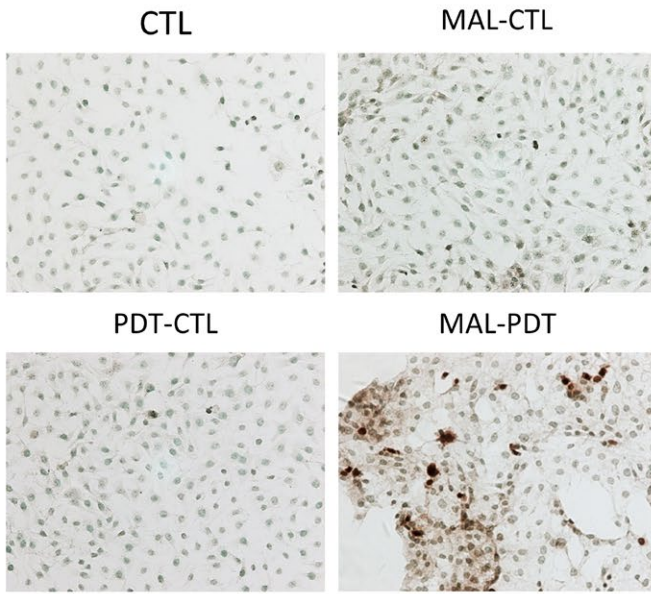


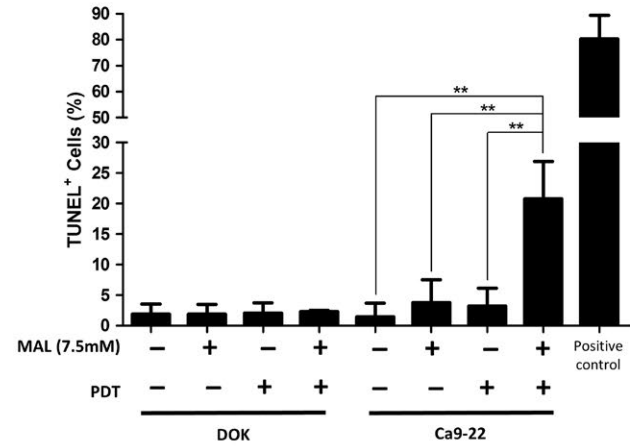
FIGURE 3 MAL-PDT stimulated caspase-associated cell death in Ca9-22 oral cancer cells. (a) The morphology of Ca9-22 cells in culture flask (magnification $\times 100$), as visualized by light microscopy before and after MAL-PDT treatment. CTL, cells without any treatment; MAL-CTL, cells treated with MAL only; PDT-CTL, cells treated with PDT only; MAL-PDT, cells treated with MAL-PDT. (b) The effect of MAL-PDT on Ca9-22 cell viability, as analyzed by the XTT assay. (c) Colonies of Ca9-22 cells were stained with crystal violet for the determination of colony numbers. (d) ROS formation in Ca9-22 cells was determined by DHE staining followed by flow cytometric analysis. (e) Apoptotic cell death in Ca9-22 cells was determined by Annexin V/PI staining followed by flow cytometric analysis. (f) The expression of caspase-associated proteins in Ca9-22 cells was analyzed by immunoblotting. (g) Apoptotic cell death in Ca9-22 cells was determined by TUNEL staining. Cells were also counterstained with methyl green (magnification: $200\times$). (h) Apoptotic cell death in oral cancer cells was determined by flow cytometry using the TUNEL assay. (i) Oral cancer tissues in buccal pouch of hamsters were stained with H&E and TUNEL. Representative photographs are shown with $\times 400$ magnification [Colour figure can be viewed at wileyonlinelibrary.com]

G

Ca9-22



H



I

Hamster cancer tissue

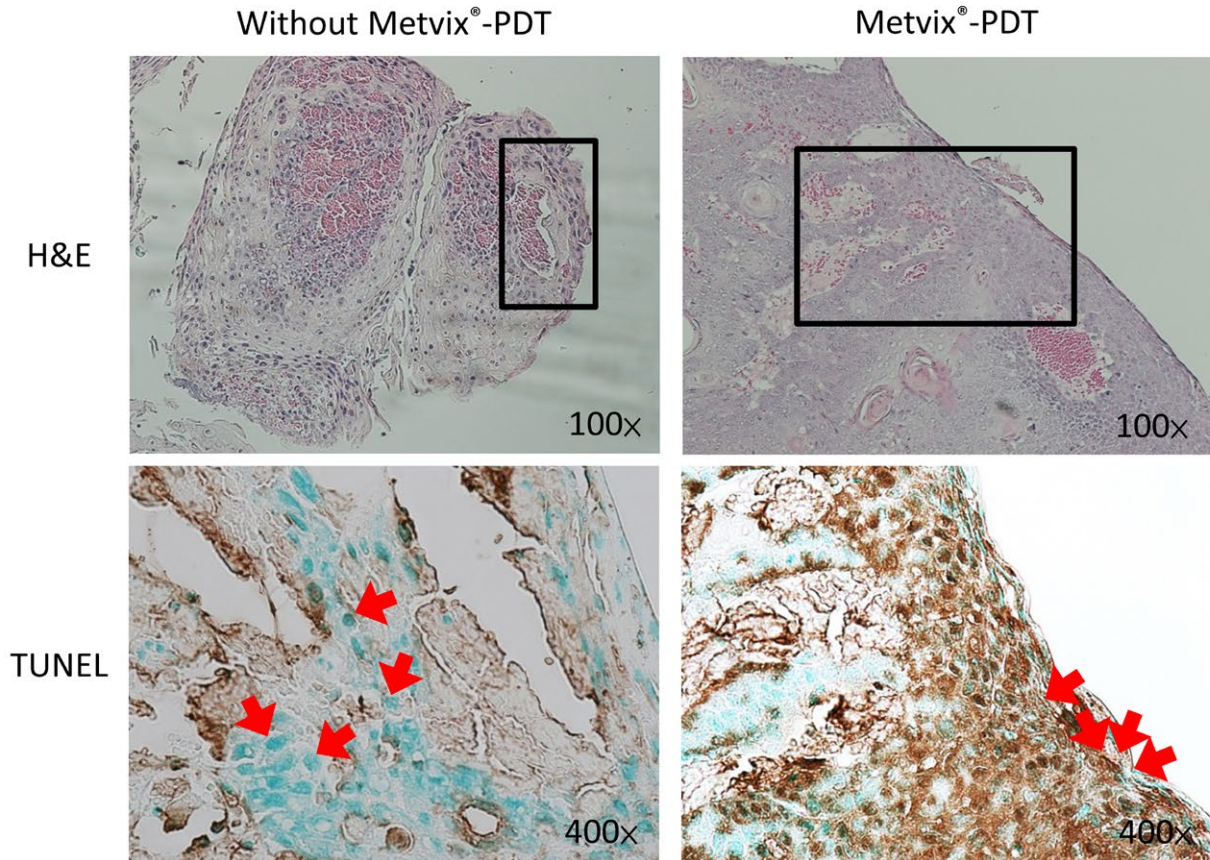


FIGURE 3 Continued

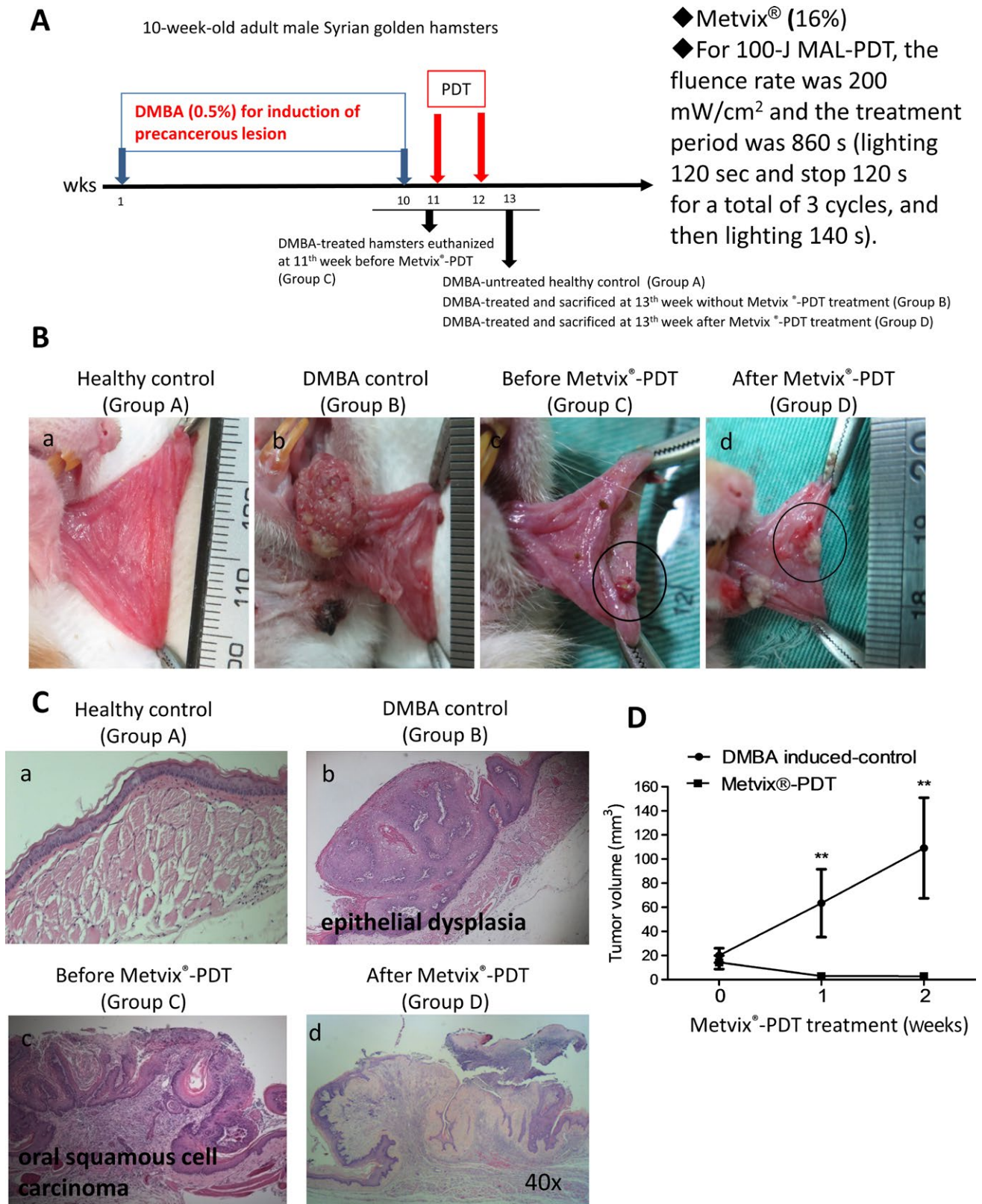


FIGURE 4 Metvix[®]-PDT suppressed the growth of oral precancerous lesions induced by DMBA. (a) The flowchart for the experimental design. (b) Pictures taken from 4 experimental groups: without DMBA induction or Metvix[®]-PDT treatment (Group A, healthy control); with DMBA induction (Group B, DMBA control); with DMBA induction but euthanized before Metvix[®]-PDT treatment (Group C, before Metvix[®]-PDT); with DMBA induction followed by Metvix[®]-PDT treatment (Group D, after Metvix[®]-PDT). (c) H&E stains from the four experimental groups are shown with $\times 40$ magnification. (d) Tumor volumes were measured and compared between DMBA control and Metvix[®]-PDT treatment groups according to the formula $\text{width}^2 \times \text{length} / 2$. The data were presented as mean \pm SD. ** $p < 0.01$, by t test [Colour figure can be viewed at wileyonlinelibrary.com]

4 | DISCUSSION

The application of PDT in oral precancerous lesions has been previously reported (Figueira & Veltrini, 2017; Saini, Lee, Liu, & Poh, 2016). However, our study provides the very first report on the application of MAL-PDT in oral precancerous lesions. Our results demonstrated that MAL-PDT decreased viability in oral precancerous cells *in vitro* and inhibited the growth of oral precancerous lesions *in vivo*, through autophagic cell death.

Although the PDT agents, ALA and MAL, depend on a similar mechanism to produce photoactive PpIX in precancerous and cancer tissues, they may differ in efficacy and tolerance. MAL has a high permeability and produces an effective and good cosmetic outcome in thicker actinic keratoses (AK) and basal cell carcinomas (BCC) (Rhodes et al., 2004; Tarstedt, Rosdahl, Berne, Svanberg, & Wennberg, 2005). Moreover, the pain score and discontinuity rate is higher in patients treated with ALA compared with MAL for actinic keratoses (Kasche, Luderschmidt, Ring, & Hein, 2006; Wiegell,

Stender, Na, & Wulf, 2003). For three common oral precancerous lesions, topical ALA is more effective for oral erythroleukoplakia (OEL) and oral verrucous hyperplasia (OVH) lesions but less effective for oral leukoplakia (OL). The different outcomes are due to the thinner keratin layer in OEL and OVH compared with OL (Chen, Yu, Lin, Cheng, & Chiang, 2012; Zhang et al., 2015).

Autophagy and apoptosis are two distinct forms of cell death, and only, the later is induced by the accumulation of reactive oxygen species (Eisenberg-Lerner, Bialik, Simon, & Kimchi, 2009; Hsieh, Athar, & Chaudry, 2009; Schaaf et al., 2016; Zhang et al., 2015). In our study, MAL-PDT only induced ROS production in oral cancer cells. In fact, our results showed that significant apoptosis only occurred in oral cancer cells, but not in oral precancerous cells. It has been well documented that PDT induces photodamage via apoptotic cell death in cancer cells, while autophagic cell death has only recently emerged as an important mechanism in PDT-induced cell death (Garg, Maes, Romano, & Agostinis, 2015; Kessel, 2015). PDT-induced autophagy may either protect or kill cancer cells. It protects

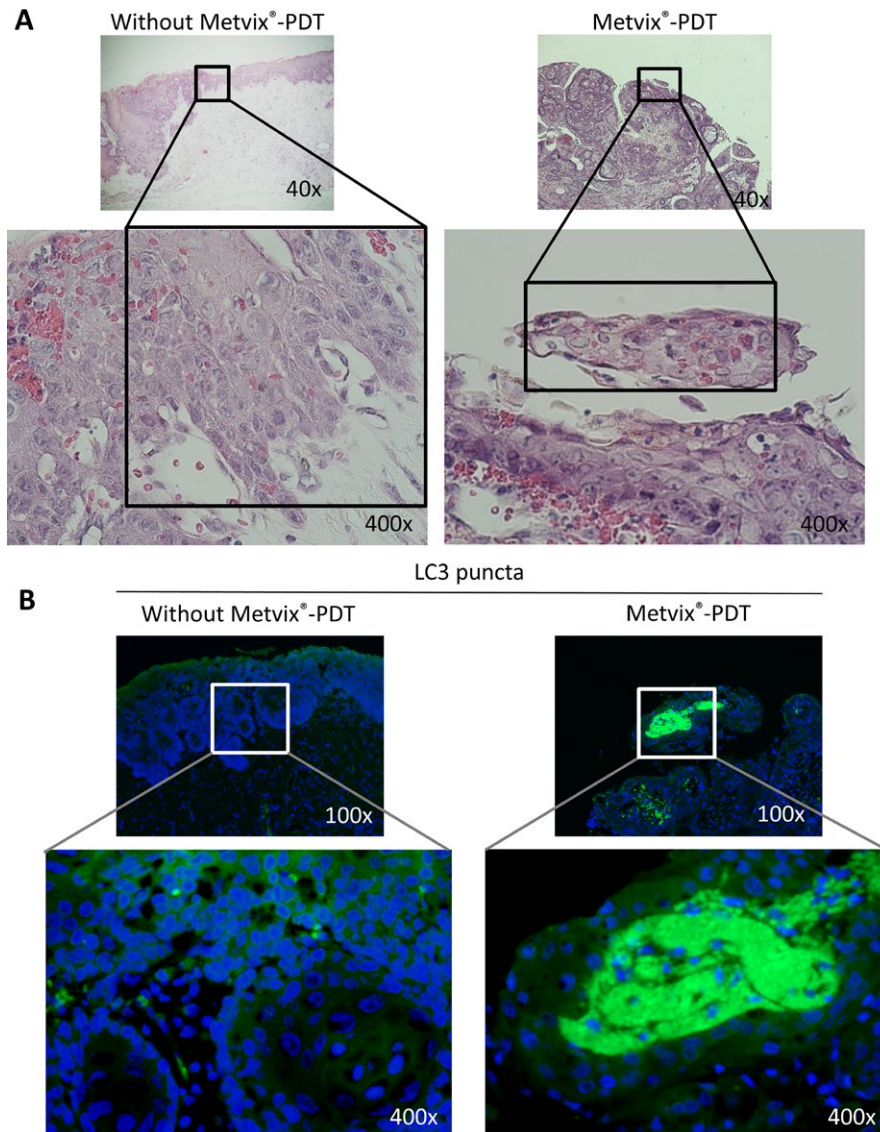


FIGURE 5 Metvix[®]-PDT-induced autophagy in DMBA-induced oral precancerous lesions. (a) Oral precancerous lesions were treated with Metvix[®]-PDT and stained with hematoxylin and eosin. Representative photographs are shown with $\times 40$ and $\times 400$ magnification. (b) Representative images of LC3 puncta (autophagosomes) in oral precancerous lesions after Metvix[®]-PDT treatment. The representative photographs are shown with $\times 100$ and $\times 400$ magnification. (c) Quantitation of LC3 puncta-positive cells in oral precancerous lesions following Metvix[®]-PDT treatment. (d) The expression of p62/SQSTM1 in oral precancerous lesions after Metvix[®]-PDT treatment, as determined by immunohistochemistry. (e) Apoptotic cells in oral precancerous lesions upon Metvix[®]-PDT treatment were determined by TUNEL assay under light microscopy. Representative photographs are shown with $\times 100$ and $\times 400$ magnification [Colour figure can be viewed at wileyonlinelibrary.com]

(c)	Lesions (N)	LC3 puncta positive(%)	LC3 puncta negative(%)	<i>p</i> -value
Metvix [®] -PDT	15	14 (93.3)	1 (6.7)	<0.0001
Without Metvix [®] -PDT	25	5 (20.0)	20 (80.0)	

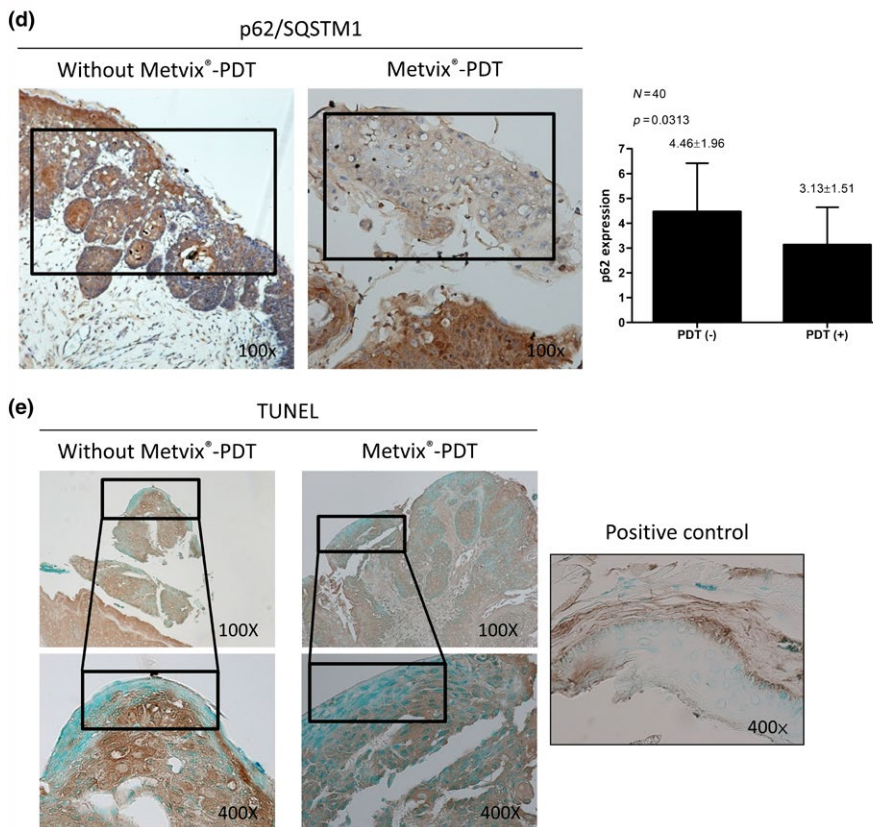


FIGURE 5 Continued

the cells if the autophagy process is complete, while it kills the cells if the process is unfinished (Garg et al., 2015; Hsieh, Pai, Hsueh, Yuan, & Hsieh, 2011; Kessel, 2015; Tanida, 2011). When absorbed into cells, photosensitizers could accumulate in many organelles such as the mitochondria, lysosomes, endoplasmic reticulum, and Golgi apparatus and may result in different outcomes (Mroz, Yaroslavsky, Kharkwal, & Hamblin, 2011). While our results showed that MAL-PDT induced autophagy in oral precancerous lesions while it induced apoptosis in oral cancer, we did not address the detailed molecular mechanisms and signaling pathways that underlie the two distinct responses, which are worthy of further studies.

While the expression of autophagy marker p62/SQSTM1 was increased in DOK cells at 4 hr after MAL-PDT treatment, it was decreased in the precancerous lesions of hamster buccal pouch at 2 weeks after MAL-PDT treatment, suggesting a time-dependent change in the expression of autophagy markers after MAL-PDT treatment.

With regard to signaling pathways underlying the autophagic cell death caused by MAL-PDT, we observed that the level of pERK1/2 in DOK cells was increased upon MAL-PDT treatment (Supporting Information Figure S4A). Co-treatment with the ERK activator U46619 reversed the cell death induced by MAL-PDT (Supporting Information Figure S4B). In contrast, co-treatment with the ERK inhibitor U0126

augmented MAL-PDT-induced cell death (Supporting Information Figure S4C). We further confirmed that the expression of pERK was significantly increased in the buccal pouch tumors after Metvix[®]-PDT treatment (Supporting Information Figure S4D). The involvement of ERK in MAL-PDT-induced autophagic cell death in DOK precancerous cells is a bit puzzling. While increased phosphorylation and activation of ERK were observed in DOK cells after MAL-PDT treatment, inhibition of ERK further increased the autophagic cell death upon MAL-PDT treatment, suggesting that ERK signaling may play a protective role against MAL-PDT-induced autophagic cell death.

In summary, our study demonstrates the inhibitory effect of MAL-PDT against oral precancerous cells and lesions, and indicates that MAL-PDT may be a potential non-invasive, well-tolerated, and convenient treatment approach for patients with oral precancerous lesions. Further mechanistic, pharmacokinetic and clinical studies are required to validate the clinical efficacy of Metvix[®]-PDT in oral precancerous lesions.

ACKNOWLEDGEMENTS

This study was supported by grant from the Ministry of Health and Welfare (MOHW107-TDU-B-212-114016, Health and welfare



surcharge of tobacco products) of Taiwan, grant from Ministry of Education for Center For Intelligent Drug Systems and Smart Bio-devices (IDS²B) from The Featured Areas Research Center Program within the framework of the Higher Education Sprout Project, and grant from Kaohsiung Medical University (KMU-Q107010), NSYSU-KMU JOINT RESEARCH (#NSYSUKMU 107-P019).

CONFLICT OF INTEREST

The authors declare that there are no conflicts of interest.

AUTHOR CONTRIBUTIONS

Y-Y Wang, Y-K Chen, S-C Hu, L-Y Xiao, W-L Huang, T-C Chi, K-H Cheng, Y-M Wang, and S-S Yuan involved in the concept and design of the experiments. Y-Y Wang, Y-K Chen, W-L Huang, and C-H Tsai involved in the performance of the experiments. Y-Y Wang, L-Y Xiao, K-H Cheng, and S-S Yuan analyzed and discussed the manuscript. Y-K Chen and S-S Yuan contributed to reagents/materials/analysis tools. Y-Y Wang, Y-K Chen, S-C Hu, L-Y Xiao, K-H Cheng, Y-M Wang, and S-S Yuan involved in the preparation of manuscript. All authors read and approved the final manuscript.

ORCID

Shyng-Shiou F. Yuan  <https://orcid.org/0000-0002-4753-788X>

REFERENCES

- Agostinis, P., Berg, K., Cengel, K. A., Foster, T. H., Girotti, A. W., Gollnick, S. O., ... Golab, J. (2011). Photodynamic therapy of cancer: an update. *CA: A Cancer Journal for Clinicians*, *61*, 250–281.
- Bicalho, L. S., Longo, J. P., Cavalcanti, C. E., Simioni, A. R., Bocca, A. L., de Santos, M. F., ... Azevedo, R. B. (2013). Photodynamic therapy leads to complete remission of tongue tumors and inhibits metastases to regional lymph nodes. *Journal of Biomedical Nanotechnology*, *9*, 811–818.
- Chen, H.-M., Yu, C.-H., Lin, H.-P., Cheng, S.-J., & Chiang, C.-P. (2012). 5-Aminolevulinic acid-mediated photodynamic therapy for oral cancers and precancers. *Journal of Dental Sciences*, *7*, 307–315.
- Chen, Y. K., & Lin, L. M. (2010). DMBA-induced hamster buccal pouch carcinoma and VX2-induced rabbit cancer as a model for human oral carcinogenesis. *Expert Review of Anticancer Therapy*, *10*, 1485–1496.
- Cohen, D. K., & Lee, P. K. (2016). Photodynamic therapy for non-melanoma skin cancers. *Cancers*, *8*(10), 90. <https://doi.org/10.3390/cancers810090>
- Eisenberg-Lerner, A., Bialik, S., Simon, H. U., & Kimchi, A. (2009). Life and death partners: Apoptosis, autophagy and the cross-talk between them. *Cell Death and Differentiation*, *16*, 966–975.
- Fargnoli, M. C., & Peris, K. (2015). Photodynamic therapy for basal cell carcinoma. *Future Oncology*, *11*, 2991–2996.
- Figueira, J. A., & Veltrini, V. C. (2017). Photodynamic therapy in oral potentially malignant disorders-Critical literature review of existing protocols. *Photodiagnosis and Photodynamic Therapy*, *20*, 125–129.
- Garg, A. D., Maes, H., Romano, E., & Agostinis, P. (2015). Autophagy, a major adaptation pathway shaping cancer cell death and anticancer immunity responses following photodynamic therapy. *Photochemical & Photobiological Sciences*, *14*, 1410–1424.
- Gaullier, J. M., Berg, K., Peng, Q., Anholt, H., Selbo, P. K., Ma, L. W., & Moan, J. (1997). Use of 5-aminolevulinic acid esters to improve photodynamic therapy on cells in culture. *Cancer Research*, *57*, 1481–1486.
- Godeny, M. (2014). Prognostic factors in advanced pharyngeal and oral cavity cancer; significance of multimodality imaging in terms of 7th edition of TNM. *Cancer Imaging*, *14*, 15.
- Guneri, P., & Epstein, J. B. (2014). Late stage diagnosis of oral cancer: Components and possible solutions. *Oral Oncology*, *50*, 1131–1136.
- Gupta, N., Gupta, R., Acharya, A. K., Patthi, B., Goud, V., Reddy, S., ... Singla, A. (2016). Changing trends in oral cancer – A global scenario. *Nepal Journal of Epidemiology*, *6*, 613–619.
- Hsieh, C. H., Pai, P. Y., Hsueh, H. W., Yuan, S. S., & Hsieh, Y. C. (2011). Complete induction of autophagy is essential for cardioprotection in sepsis. *Annals of Surgery*, *253*, 1190–1200.
- Hsieh, Y. C., Athar, M., & Chaudry, I. H. (2009). When apoptosis meets autophagy: Deciding cell fate after trauma and sepsis. *Trends in Molecular Medicine*, *15*, 129–138.
- Hsu, Y. C., Yang, D. F., Chiang, C. P., Lee, J. W., & Tseng, M. K. (2012). Successful treatment of 7,12-dimethylbenz(a)anthracene-induced hamster buccal pouch precancerous lesions by topical 5-aminolevulinic acid-mediated photodynamic therapy. *Photodiagnosis and Photodynamic Therapy*, *9*, 310–318.
- Kasche, A., Luderschmidt, S., Ring, J., & Hein, R. (2006). Photodynamic therapy induces less pain in patients treated with methyl aminolevulinic acid compared to aminolevulinic acid. *Journal of Drugs in Dermatology: JDD*, *5*, 353–356.
- Kessel, D. (2015). Autophagic death probed by photodynamic therapy. *Autophagy*, *11*, 1941–1943.
- Kim, M., Jung, H. Y., & Park, H. J. (2015). Topical PDT in the treatment of benign skin diseases: Principles and new applications. *International Journal of Molecular Sciences*, *16*, 23259–23278.
- Mroz, P., Yaroslavsky, A., Kharkwal, G. B., & Hamblin, M. R. (2011). Cell death pathways in photodynamic therapy of cancer. *Cancers*, *3*, 2516–2539.
- Rhodes, L. E., de Rie, M., Enstrom, Y., Groves, R., Morken, T., Goulden, V., ... Wolf, P. (2004). Photodynamic therapy using topical methyl aminolevulinic acid vs surgery for nodular basal cell carcinoma: Results of a multicenter randomized prospective trial. *Archives of Dermatology*, *140*, 17–23.
- Rigual, N. R., Shafirstein, G., Frustino, J., Seshadri, M., Cooper, M., Wilding, G., ... Henderson, B. (2013). Adjuvant intraoperative photodynamic therapy in head and neck cancer. *JAMA Otolaryngology Head & Neck Surgery*, *139*, 706–711.
- Saini, R., Lee, N. V., Liu, K. Y., & Poh, C. (2016). Prospects in the application of photodynamic therapy in oral cancer and pre-malignant lesions. *Cancers*, *8*(9), 83. <https://doi.org/10.3390/cancers8090083>
- Schaaf, M. B., Keulers, T. G., Vooijs, M. A., & Rouschop, K. M. (2016). LC3/GABARAP family proteins: Autophagy-(un)related functions. *The FASEB Journal*, *30*, 3961–3978.
- Shklar, G., Eisenberg, E., & Flynn, E. (1979). Immunoenhancing agents and experimental leukoplakia and carcinoma of the hamster buccal pouch. *Progress in Experimental Tumor Research*, *24*, 269–282.
- Tanida, I. (2011). Autophagosome formation and molecular mechanism of autophagy. *Antioxidants & Redox Signaling*, *14*, 2201–2214.
- Tarstedt, M., Rosdahl, I., Berne, B., Svanberg, K., & Wennberg, A. M. (2005). A randomized multicenter study to compare two treatment regimens of topical methyl aminolevulinic acid (Metvix)-PDT in actinic keratosis of the face and scalp. *Acta Dermato-Venereologica*, *85*, 424–428.
- Thome, M. P., Filippi-Chiela, E. C., Villodre, E. S., Migliavaca, C. B., Onzi, G. R., Felipe, K. B., & Lenz, G. (2016). Ratiometric analysis of acridine orange staining in the study of acidic organelles and autophagy. *Journal of Cell Science*, *129*, 4622–4632.

- Tierney, E. P., Eide, M. J., Jacobsen, G., & Ozog, D. (2008). Photodynamic therapy for actinic keratoses: Survey of patient perceptions of treatment satisfaction and outcomes. *Journal of Cosmetic and Laser Therapy, 10*, 81–86.
- van Straten, D., Mashayekhi, V., de Bruijn, H. S., Oliveira, S., & Robinson, D. J. (2017). Oncologic photodynamic therapy: Basic principles, current clinical status and future directions. *Cancers, 9*(12), 19. <https://doi.org/10.3390/cancers9020019>
- Wang, I., Bendsoe, N., Klinteberg, C. A., Enejder, A. M., Andersson-Engels, S., Svanberg, S., & Svanberg, K. (2001). Photodynamic therapy vs. cryosurgery of basal cell carcinomas: Results of a phase III clinical trial. *The British Journal of Dermatology, 144*, 832–840.
- Wen, X., Li, Y., & Hamblin, M. R. (2017). Photodynamic therapy in dermatology beyond non-melanoma cancer: An update. *Photodiagnosis and Photodynamic Therapy, 19*, 140–152.
- Wiegell, S. R., Stender, I. M., Na, R., & Wulf, H. C. (2003). Pain associated with photodynamic therapy using 5-aminolevulinic acid or 5-aminolevulinic acid methylester on tape-stripped normal skin. *Archives of Dermatology, 139*, 1173–1177.
- Yamamoto, M., Fujita, H., Katase, N., Inoue, K., Nagatsuka, H., Utsumi, K., ... Ohuchi, H. (2013). Improvement of the efficacy of 5-aminolevulinic

acid-mediated photodynamic treatment in human oral squamous cell carcinoma HSC-4. *Acta Medica Okayama, 67*, 153–164.

- Zhang, L., Wang, K., Lei, Y., Li, Q., Nice, E. C., & Huang, C. (2015). Redox signaling: Potential arbitrator of autophagy and apoptosis in therapeutic response. *Free Radical Biology and Medicine, 89*, 452–465.

SUPPORTING INFORMATION

Additional supporting information may be found online in the Supporting Information section at the end of the article.

How to cite this article: Wang Y-Y, Chen Y-K, Hu C-S, et al. MAL-PDT inhibits oral precancerous cells and lesions via autophagic cell death. *Oral Dis.* 2019;25:758–771. <https://doi.org/10.1111/odi.13036>